

# **Cardiac related Complexity Changes of Zero-Quantum Coherence (ZQC) signals in Brain MR Imaging: Comparison between Young and Older Healthy Volunteers**

David López Pérez<sup>1,2</sup>, Arun L.W. Bokde<sup>3</sup> & Christian Kerskens<sup>2</sup>

<sup>1</sup>Institute of Psychology, Polish Academy of Sciences, Warsaw, Poland

<sup>2</sup>Institute of Neuroscience, Trinity College, Dublin, Ireland

<sup>3</sup>Trinity College Institute of Neuroscience and Cognitive Systems Group, Discipline of Psychiatry, School of Medicine, Trinity College Dublin, Ireland

\* Correspondence:

David López Pérez, [d.lopez@psych.pan.pl](mailto:d.lopez@psych.pan.pl), Institute of Psychology, Polish Academy of Sciences, Jaracza, 1, 00-378 Warsaw, Poland, tel. 0048 666331709

# Abstract

There are multiple magnet resonance imaging (MRI) based approaches to studying the ageing brain. Getting older affects both the structure of the brain and our cognitive capabilities but there is still no solid evidence on how ageing influences the mechanisms underlying the MRI signal. Here, we apply a recently developed long-range zero-quantum coherence (ZQC) weighted MRI sequence that was found to be sensitive to wakefulness. We found that the complexity of the signal time curve is also affected by age. While comparing young and old participants, we found qualitative and quantitative evidence that the dynamics of these quantum fluctuations undergo strong changes with age. Finally, we study how differences in long-range ZQC relate with measures from different cognitive batteries, suggesting that long-range ZQC may be key for cerebral dynamics and cognitive functioning. The profound sensitivity for dynamic changes shows the potential of long-range ZQC and its underlying physiological mechanism with clinical relevance for all neurovascular diseases.

Keywords: Complexity, Quantum Coherence, Cognitive Ageing, MRI, Consciousness

# Introduction

It is well established that normal ageing has cascading effects on many cognitive domains and affects the brain at multiples levels ranging from sub- to macro-cellular (e.g., [1,2]). For instance, older adults have particular difficulties with episodic memory [3], working memory (e.g., [4]) or are slower processing different stimuli (e.g., [5]). At the same time, some aspects of cognition are maintained, such as semantic memory [6] or emotional regulation[7]. However, the cerebral mechanisms that underlie this better or lesser performance are still poorly understood [8]. A vast amount of studies have tried to link these structural changes to age differences in cognitive function. Magnetic resonance imaging (MRI) based methods have been mainly used to study changes in the ageing brain. Among the various MRI methods, functional MRI (fMRI), with more than 10000 published papers, is probably the one more widely applied (e.g., [9]). The blood oxygen level-dependent (BOLD) signal obtained from fMRI is an indirect index of neural activity and reflects small metabolic changes in deoxyhaemoglobin concentrations that take place when a specific region of the brain is active [10]. These responses have been found to be similar in both young and older adults [8], but in some cases, the magnitude of the BOLD response was reduced in older adults (e.g., [11]) while sometimes was increased (e.g., [12]). The former is often related to cognitive deficits in older adults (e.g., [13]), while the latter is often interpreted as compensatory (e.g., [14]) or as a reduction in the selectivity of responses [15]. Independently of the direction of these magnitude variations, changes in cerebral vasculature with age (e.g., [16]), are somehow expected to influence the mechanisms underlying the fMRI signal. Although still unknown, these changes should be related to differences in cognitive performance, but no substantial evidence has been found so far.

This comes as a surprise because heart functions also alter with age which should, in turn ,affect cerebral blood flow. Even more, it is well known that several heartbeat-related effects influence conscious perception where the cardiac cycle may impact the perception of visual or auditory stimuli (e.g., [17]). The existence of heartbeat-evoked potential (HEP) in general is strong

evidence that the heartbeat influences neuronal functions [18]. In a recent study, Kerskens and López Pérez [19] discovered phase transitions in the brain tissue stimulated by the heartbeat which may shed light into the underlying mechanism of HEPs and heartbeat related conscious perceptions. Phase transition are accompanied with order changes in the molecular structures of brain tissue which may play essential roles for long-range signalling between brain regions. MRI is generally sensitive for phase transition which is reflected in T1 and T2 relaxation changes but Kerskens and López Pérez [19] focussed on exotic phase transition with long-range effects which can be detected with multiple-quantum coherence (MQC). Using a MRI time-series acquisition, they found fluctuations in the brain, whose underlying mechanism was related to the zero-quantum coherence (ZQC) properties of the magnetic resonance signal [19]. Those fluctuations were evoked by the heartbeat only during wakefulness, which underpins its importance for consciousness and cognition.

Quantum coherence has not traditionally been considered as a powerful tuning element for enhancing or explaining functions in biology [20]). However, a growing body of literature has recently demonstrated that quantum coherence in living organisms exists and it is itself essential for their functioning (e.g., [21,22]). With the recent rise of the field of quantum biology, it has been suggested that quantum phenomena might also influence brain activity and affect its cognition [23]. However, it is important to consider the brain itself as a non-linear dynamical complex system, whose activity may vary if the system changes [23]. As a consequence, these quantum fluctuations that arise from the interaction between the brain and the heart would be high-dimensional, and thus, the complexity of the system (i.e., its ability to adapt and function in an ever-changing environment) would also be high-dimensional [24]. Recent studies have shown that high complexity is characteristic to healthy systems and that can degrade as a consequence of disease or ageing [25]. Thus, if this mechanism is vital for cerebral dynamics, the complexity of these fluctuations needs to be kept high and any variation on the dynamics with age should affect the complexity of the system.

In this paper, we want to study, for the first time, how the dynamical complexity of the long-range quantum coherence signal may vary with age. To characterise these fluctuations as entirely as possible, we use a broad range of dynamical systems measures. First, we applied Recurrence Quantification Analysis (RQA; [26]), which is an increasingly popular method to analyse dynamical changes of behaviour in complex systems. This concept has been used to study physiological signals [27,28] heart rate variability ([25] or the dynamics of heart rhythm modulation [29]. The main benefits of RQA in comparison to standard analysis resides in its sensitivity to small changes in the system dynamics [25]. Secondly, we employed MultiFractal Detrended Fluctuation Analysis to extract the fractal properties of the signal (MFDFA; [29]). Multifractal Analysis is another efficient non-linear method to study the fractal scaling properties and long-range correlations of noisy signals ([24]; for a review see [31]). Fractal differences as a consequence of ageing have been found between monofractal or multifractal signals in EEG [32] or due to HRV changes [33]. Finally, we relate these measures with different cognitive batteries and show that those quantum fluctuations may be key for cerebral dynamics and cognitive functioning.

## **Methods**

### ***Participants***

60 subjects (29 participants between 18 and 29 years old, and 31 participants over 65 years old) were scanned with the protocols approved by the St. James Hospital and the Adelaide and Meath Hospital, incorporating the National Children Hospital Research Ethics Committee. All participants were adults recruited for a larger study [34-36] and came from the greater Dublin area.

All participants underwent the Cambridge Neuropsychological Test Automated Battery (CANTAB; [37]) which has been used to detect changes in neuropsychological performance and include tests of working memory, learning and executive function; visual, verbal and episodic memory; attention, information processing and reaction time; social and emotion recognition,

decision making and response control. The CANTAB scores were normalised for age and IQ.

Particularly, the following subtest were administered:

- The Paired Associate Learning Test is a measure of episodic memory where boxes are displayed on the screen, and each one has a distinct pattern. The boxes are opened in random order, revealing the pattern behind the box. In the test phase, patterns are individually displayed in the centre of the screen, and participants must press the box that shields the respective pattern.

- Pattern Recognition Memory is a test of visual pattern recognition memory in which the participant is presented with a series of visual patterns, one at a time, in the centre of the screen. In the recognition phase, the participant is required to choose between a pattern they have already seen and a novel pattern. In this phase, the test patterns are presented in the reverse order to the original order of presentation. This is then repeated, with new patterns. The second recognition phase can be given either immediately (immediate recall) or after a delay (delay recall).

- The Spatial Working Memory Test assesses spatial working memory in which boxes are presented on the computer screen and hidden behind one of the boxes is a yellow circle. Participants must find the box where the yellow circle is located. As the task progresses, the number of boxes on the screen increases. We analysed the spatial working memory strategies (i.e., the number of times participants begin a new search strategy from the same box).

Moreover, participants performed the trail making test (TNT; [38]) which is a neuropsychological test of visual attention and task switching. TNT test that can provide information about visual search speed, scanning, speed of processing, mental flexibility, as well as executive functioning [39].

### ***MRI data acquisition***

Each participant was imaged in a 3.0 T Philips whole-body MRI scanner (Philips, The Netherlands) using a standard single-shot GE EPI sequence operating with a 8-channel array

receiver coil in all cases. The parameters of the EPI time-series sequence were as follows: Flip angle = 30°, TR = 60 ms and the TE = 18 ms with a voxel size was 3.5 x 3.5 x 3.5 mm, matrix size was 64 x 64, SENSE factor 3, bandwidth readout direction was 2148 Hz and saturation pulse was 6 ms with 21 mT/m gradient strength. The imaging slice was set coronal above the ventricle to avoid pulsation effects (see Figure 1 for example). In addition, two saturation slices of 5 mm in thickness were placed parallel to the imaging slice (15 mm above and 20 mm below). These slabs were applied to introduce asymmetrical magnetic gradient scheme for the ZQC contrast (for a full description see [19]). Additional scans without the saturation slabs using the same imaging parameters were carried out which had two effects on the ZQC; a change of the angulation between the asymmetric gradient field and the main magnet field towards the magic angle and a lengthening of the ZQC correlation distance. As a result, ZQC were strongly reduced leaving only higher-order coherence in the time-series and very long-distance quantum coherence. In this manuscript, we refer to these scans as the SQC weighted signal to differentiate it from the ones that contain stronger ZQC effects (i.e., ZQC weighted signal). The average angulation of the imaging slice was  $14.76 \pm 5.65$  degrees and for each participant the angulation was always the same during the acquisition with the slab and without it.

---

Insert Figure 1 Here

---

Anatomical MRI images in all studies included a high-resolution sagittal, T1-weighted MP-RAGE (TR = 2.1 s, TE = 3.93 ms, flip angle = 7°). The ZQC sequence was acquired after the resting-state fMRI part of the session. The radiographer always contacted the participants before the acquisition to make sure that they were awake. This step is important given that the ZQC signal has been suggested to be sensitive to changes in wakefulness of the participant [19].

### ***Signal Preprocessing***

All calculations were developed in a Dell Optiplex 790 with 12 Gb RAM using Matlab 2017a (The MathWorks Inc., Natick, MA, 2017). Since motion correction could not be applied

due to the single slice nature of the experiment, average time-series were visually inspected in search for irregularities which were manually removed from the analysis leaving the rest of the time-series unaltered. In addition, the data was not smoothed to avoid removing low frequencies which may lead to the loss of information [40]. Manual segmentation was used to create a mask to remove cerebrospinal fluid (CSF) contributions which were later eroded to avoid partial volume effects at the edges. The first 100 scans were removed to avoid signal saturation effects.

### ***Recurrence Quantification Analysis***

We used Recurrence Quantification Analysis (RQA) to analyse the dynamical temporal characteristics of the MRI signals. RQA quantifies the repeated occurrences of a given state of a system (i.e., recurrences) by analysing the different structures present in a recurrence plot, which is a graphical representation of the recurrences in the dynamical system [26]. In our analysis, we considered the following RQA measures [41]:

- Determinism (Det): it represents a measure that quantifies repeating patterns in a system and it is a measure of its predictability. Regular, periodic signals, such as sine waves, have higher DET values, while uncorrelated time-series cause low DET.
- Mean Line (MeanL): it is the average length of repeating patterns in the system. It represents the mean prediction time of the signal, a measure of chaos or divergence from an initial point.
- Entropy (Ent): it is the Shannon entropy of the distribution of the repeating patterns of the system. If a signal has high entropy it exhibits diversity in short- and long-duration periodicities.
- Laminarity (Lam): it determines the frequency of transitions from one state to another, without describing the length of these transition phases. It indexes the general level of persistence in some particular state of one of the time-series [42].



- Trapping Time (TT): it represents the average time the system remains on a given state and it is a measure of the stability of the system. It was calculated here using the *tt* function from the CRP Toolbox for Matlab [43].
- Maximum Line (MaxL): it is the largest Lyapunov exponent of a chaotic signal, which gives the longest time spent in a single state by the system [44].

Three critical parameters need to be set to calculate the recurrence plots. First, the smallest sufficient embedding dimension was determined using the *fnn* function [45] within the CRP Toolbox (Marwan, N.: Cross Recurrence Plot Toolbox; [46], for MATLAB, Ver. 5.22 (R31.2), <http://tocsy.pik-potsdam.de/CRPtoolbox/>). This function estimates the minimum embedding dimension where the false nearest neighbours vanish. We applied the *fnn* to all time-series and obtained an average value of 15, which agrees with the typical values recommended for biological signals [27]. The second parameter is the delay which we calculated using the *mi* function from the CRP Toolbox [46,47]. This function finds the non-linear interrelations in the data and determines which delay fulfils the criterion of independence. In the same way as the embedding dimension, we applied the *mi* function to all time-series and we obtained an average value of 3. Finally, several criteria have been suggested for the choice of the recurrence threshold [48]. Here, we adapted the radius for each time-series using the embedding dimension and delay computed together with a recurrence rate sufficiently low (i.e.,  $RR = 3\%$ ) [43]. Additional parameters in the RQA calculations were Euclidean normalisation for each time-series and minimum line length equal to 2.

### ***Multifractal Detrended Fluctuation Analysis***

In biological systems, the coupling between different systems often exhibits different spatial and temporal scales and hence its complexity is also multi-scale and hierarchical [24]. Thus, to analyse the scale-invariant properties of the MRI segments and its changes with age we used Multifractal Detrended Fluctuation Analysis (MFDFA). To do so, we first, calculated the

multifractal spectrum,  $D$ , of each time-series using the MFDFA Matlab Toolbox [30]. The multifractal spectrum identifies the deviations in fractal structure within time-periods with large and small fluctuations [30]. Each spectrum was computed using a window length with a minimum value of 2 and a maximum value of half the length of the time-series. The  $q$ -order statistical moments were chosen between -11 and 11 and divided into 21 steps (see further description in [30]).

From each fractal spectrum, two parameters were calculated, i.e., the width of the spectrum  $W$  and the position of the spectrum maxima  $H$ . The width  $W$  is calculated by subtracting the lower part of the spectrum,  $h$ , to the upper part of the spectrum,  $h$  [30, 33, 49]. A small width indicates that the time-series has fewer singularities and tends to be more monofractal. Finally, the  $H$  parameter represents the value  $h$  in which the singularity spectra has its maximum  $h(D)$  [33]. The position of  $h$  moves to higher values when the stronger singularities are present. Highly deterministic signals can often be explained by a lower number of fractal dimensions and are characterised by smaller  $W$  and  $H$  due to a decrease in the number of singularities.

### ***Statistical Analysis***

Before any statistical analysis all variables were converted to z-scores. Those participants having z-scores larger than 3 standard deviations in three non-linear parameters or more were rejected from the analysis. In total only 1 participant in the old group was removed. Independent  $t$ -tests were computed to test differences between the RQA and fractal measures of the average MRI signals in both groups. Inspection of Q-Q Plots was carried out to all the measures to check if the data were normally distributed. Additionally, Levene's test for equality of variances was applied and in those cases where this assumption was violated, a  $t$  statistic not assuming homogeneity of variance were computed on these measures. Finally, a linear regression between the non-linear measures and the participants age were performed.

## Results

### *The ZQC weighted signals*

Examples of the ZQC-weighted signals and their Fourier transform of both age groups are shown in figure 2a-h. As it can be seen, strong cardiac signal fluctuations are resolved only in the average time-series of young subjects (Figure 2a and 2c) while in older subjects the strong cardiac signals are diminished (Figure 2e and 2g). The frequency spectra of the time-series (Figure 2b, 2d, 2f and 2h) showed the strongest cardiac frequencies for the young group, while in the older group, however, the spectra show stronger harmonics, envelope waves or both, in addition to the weaker cardiac frequencies. These envelope waves have a beat frequency of the (cardiac frequency)/n, where n takes values of (2,3,4,6,9 ...). These results are consistent over most subjects.

---

Insert Figure 2 Here

---

### *Non-linear dynamics of the ZQC weighted signal*

We also tested how the non-linear dynamics varied in the ZQC weighted time-series in all participants (see Supplementary Results for the SQC results). At a group level all the RQA parameters but the DET were statistically significantly higher in the old group in comparison to the young one (see Table 1 for group averages): MeanLine ( $t(57) = 2.23, p = .02; d = .58$ ), MaxLine ( $t(57) = 2.81, p = .007; d = .73$ ), Ent ( $t(57) = 2.62, p = .01; d = .68$ ), Lam ( $t(57) = 3.68, p = .001; d = 0.96$ ) and TT ( $t(57) = 4.57, p < .001; d = 1.19$ ) and Det ( $t(57) = 1.23, p = .22; d = .32$ ).

---

Insert Table 1 Here

---

Likewise, the fractal properties of the ZQC weighted signal in the old group were statistically higher in  $W(t(57) = 5.44, p < .001; d = 1.41)$  and  $H(t(57) = 3.53, p = .001; d = .92)$  in comparison to the young group, suggesting a more chaotic behaviour in the old population.

## *Are group differences coming from movement or cognitive differences?*

Since the ZQC effects are sensitive to movement, we explored the relationship between the non-linear parameters and motion quality control variables from the rs-fMRI as a proxy for potential average movement of the participant. Although the information was not available for the young group, there were no significant correlations between these measures (see Table 2) or in other words, the non-linear dynamics in the old cohort were not worsened by motion.

---

Insert Table 2 Here

---

Finally, we explored any possible relation to cognitive measures and tests performed during the study. CANTAB scores showed consistent negative correlations and trends (see Table 3, Figure 3) between visual memory scores (pattern recognition memory and working memory) and the RQA parameters while no correlations arose with the TNT scores. Consistently, young participants that showed higher complexity (i.e., smaller non-linear parameters) also had better cognitive scores. Altogether, there were significant changes with ageing but even more with these cognitive scores which suggest that the ZQC signal may be related to aspects of cognition.

---

Insert Table 3 Here

---



---

Insert Figure 3 Here

---

## **Discussion**

In this paper, we have analysed if the dynamical complexity of long-range quantum coherence fluctuations in the brain tissue varies with age. While comparing two populations, we presented qualitative evidence that the strong cardiac constant fluctuations are more likely resolved for the younger subjects while for the older ones, the strong cardiac effect is diminished. Non-linear analyses confirmed this effect and showed quantitative differences between both age groups, which were related to variations in complexity and chaos of the measured signals. Particularly, the higher complexity of ZQC weighted signal was related to better cognitive performance in some of

the CANTAB scales, which was not correlated to age. Altogether, this may suggest that the long-range quantum fluctuations may be sensitive to ageing, cognition or even differences in wakefulness.

The changes in the ZQC weighted signal were manifold, varying in shape, amplitude and frequency (see Figure 2). In particular, older participants possessed a higher number of frequencies as well as a decrease in the size and number of the cardiac bursts. On the other hand, the younger group was characterised by roughly constant bursts and clear cardiac frequencies with almost no harmonics. Initially, one may think that differences between both groups can be due to old participants moving more inside the scanner. In fact, Kerskens and López Pérez [19] reported that during hyperventilation inside the scanner the ZQC effect entirely vanished due to increased movement. Although the information was not available for the young group, motion quality control variables from an fMRI study within the same session did not correlate with any of the non-linear parameters (see Table 2). Thus, we can conclude that the dynamics in the older cohort were not worsened by motion. Regardless of this, future studies using the sequence should try to minimise the effect of movement during the data acquisition (e.g., adding extra cushions to hold the head) which might help improve the intensity of the quantum effect [19].

A second possibility is that the ZQC signal declines with changes in cognition or age. To check that, we first quantified the apparent differences between both groups using non-linear time-series analyses to determine changes in the dynamics of the MRI signals. First, we applied Recurrence Quantification Analysis (RQA), which was proven to be sensitive to small changes in the system dynamics and a powerful discriminatory tool to detect significant differences between both age groups (see Supplementary files for further discrimination analysis between both groups based on these measures). All the RQA measures (see Table 1 and Supplementary Table 1) were lower in the young group in comparison to the older group in both types of MRI signals, suggesting differences in the complexity of the underlying signal dynamics in both populations. Second, we applied fractal analysis to study the fractal scaling properties and long-range correlations of the

signals. We showed an increase in the number of singularities with age, which is characterised by an increase in the width and position of the spectral maxima [30,50]. These differences were supported by the RQA entropy which denotes the Shannon entropy of the histogram of the lengths of diagonal segments and thus indicates the complexity of the deterministic structure of the system [25]. This increase in the chaoticity of the signal is only visible when the quantum effects are measured since no differences were found between the fractal parameters in the control condition (see Supplementary Table 1). Additionally, exploratory analyses showed an incremental tendency with age (see Supplementary Figures 1 and 2), but these results need to be replicated with an independent sample where a whole range of ages gets included. Altogether, we have shown that evoked by the heart and under special conditions long-range quantum fluctuations can be measured (for more details see [19]) and that they decline with age.

The ZQC declines with age but does it relate to cognition? Our results are in line with recent studies indicating that higher complexity in a system is a feature of healthy dynamics [25] or higher degree of functional specialisation and integration in brain dynamics [51] and that this complexity declines with disease and age (e.g., [52]). In fact, we observed some significant negative correlations between CANTAB scores, and RQA measures (see Table 3), where lower scores (i.e., higher complexity) were related to better cognitive scores. Particularly significant were the relations with pattern recognition memory and working memory subscales, suggesting a link between the ZQC signal and short-term memory abilities. A potential explanation why the ZQC signal was correlated to pattern recognition memory and spatial working memory is that the acquisition slice was roughly located in parietal and posterior cingulate regions and these are areas associated with these cognitive domains (e.g., [53,54]). Paired associates learning, however, is a hippocampus-based task [55] and therefore one would not expect to find a correlation with the measured signal. Besides, fMRI studies have shown that healthy old adults present higher activity levels in some brain regions during the performance of cognitive tasks and these changes coexist with disrupted connectivity (for a review see [56]). However, to the best of our knowledge, there

are not fMRI-based signals that are able to predict these CANTAB scores consistently. This is especially surprising since the ZQC signal represents the average over the imaging slice and is a very rough and functional measurement. More importantly, the pattern recognition memory and working memory subscales that were strongly correlated with the non-linear parameters did not correlate with age (see Supplementary Table 3), which emphasises the sensitivity of the ZQC signal to cognitive changes. Thus we believe that these fluctuations, which originated from exotic phase transitions over the entire brain, may be an essential global physiological effect for understanding cerebral regulation and have clinical relevance for all neurovascular diseases.

Altogether, these results provide further evidence of the existence of quantum fluctuations in the brain tissue. However, several limitations arise in this study. First, the acquisition protocol applied to obtain the ZQC weighted signal requires fast repetition times in combination with magnetisation transfer effects, which limits the number of imaging slices to just one. The use of one imaging slice complicates the study of particular areas and it could induce variability in the results across all the participants even when the position of the imaging slice is carefully planned. As a consequence, different slices should be acquired to study a larger region and improve the comparison between groups. Some approaches could be used to overcome this limitation. For example, next-generation MRI systems can acquire three or more imaging slabs by means of Multi-band excitation [57] with the same time resolution. A second improvement can be achieved with the increase in the number of channels in the receiver coil, which allow the acquisition of data with shorter repetition times and better signal to noise ratio. Future research should focus on expanding the sequence protocol to be able to cover larger brain areas that would allow the use of the sequence in a wide range of studies. Secondly, differences in wakefulness among participants and between groups may have impacted the results. Kerskens and Lopez Pérez [19] showed how a participant that reported falling sleep during testing presented a sharp signal change during testing. Despite the fact that the radiographer was checking that they were awake before the data acquisition, under these conditions (i.e., testing in a supine position inside a dark room with no

specific instructions but to remain still) participants in the older group are more likely to feel sleepy, thus potentially affecting their wakefulness. Finally, the group sizes in this study were small and the results need to be considered preliminary. Further research is needed to confirm these findings.

## Conclusions

We have shown that evoked by the heart and under special conditions long-range quantum coherence can be detected and measured. Here, we provide further evidence not only of the existence of long-range quantum coherence in the brain tissue but also that it is sensitive to ageing and cognition. We showed qualitatively and quantitatively that these fluctuations worsen with age and that their decline is related to a decrease in the complexity of the quantum phenomenon. Consistent with the idea that higher complexity is related to healthier dynamics, our quantum phenomena showed higher complexity in the younger population. Altogether, the long-range quantum coherence is a promising biomarker that needs to be tested in larger and more diverse populations with clinical relevance for all neurovascular diseases.

## Acknowledgements

We would like to thank Elizabeth G. Kehoe and Dervla Farrell for assistance in acquiring the data, the Trinity College's IT Research, Sojo Joseph for carrying out the imaging protocols for all participants and Edyta Stanaszek for reading earlier versions of the manuscript. This work was supported by Science Foundation Ireland (SFI-11/RFP.1/NES/3051), the Science Foundation Ireland Stokes Programme (07/SK/B1214a), from the European Regional Development Fund via the Interregional 4A Ireland Wales Programme 2007–2013 and Trinity College Institute of Neuroscience. This project has received additional funding from the Institute of Psychology, Polish Academy of Sciences.



## Conflict of Interest

The authors have declared no conflict of interest

## References

- [1] Salat, D. H., Buckner, R. L., Snyder, A. Z., Greve, D. N., Desikan, R. S. R., Busa, E., Morris, J. C. Dale, A. M. & Fischl, B. (2004) Thinning of the Cerebral Cortex in Aging, *Cerebral Cortex*, Volume 14, Issue 7, July, Pages 721–730, <https://doi.org/10.1093/cercor/bhh032>
- [2] Allen, J. S., Bruss, J., Brown, C. K., & Damasio, H. (2005). Normal neuroanatomical variation due to age: The major lobes and a parcellation of the temporal region. *Neurobiology of Aging*, 26(9), 1245–1260. <https://doi.org/10.1016/j.neurobiolaging.2005.05.023>
- [3] Craik, F.I.M. & Bosman, E.A. (1992) In: *Gerontechnology: Proceedings of the First International Conference on Technology and Aging*. Bouma H, Graafmans J, editors. IOS Press; pp. 79–92.
- [4] Balota, D.A., Dolan P.O. & Duchek J.M. (2000). In: *The Oxford Handbook of Memory*. Tulving E., Craik F., editors. Oxford University Press; pp. 395–410.
- [5] Salthouse, T.A. (1996). The processing-speed theory of adult age differences in cognition. *Psychol Rev.* ;103:403–428.
- [6] Laver, G.D. (2009). Adult aging effects on semantic and episodic priming in word recognition. *Psychol Aging* ;24:28–39.
- [7] Carstensen LL, et al. (2011) Emotional experience improves with age: evidence based on over 10 years of experience sampling. *Psychol Aging* ;26:21–33.
- [8] Grady, C. (2012). Trends in Neurocognitive Aging. *Nature Reviews. Neuroscience*, 13(7), 491–505. <https://doi.org/10.1038/nrn3256>

- [9] Tsvetanov, K.A., Henson, R.N., & Rowe, J.B. (2019). Separating vascular and neuronal effects of age on fMRI BOLD signals. *arXiv: Neurons and Cognition*.
- [10] Ogawa, S., Lee, T. M., Kay, A. R., & Tank, D. W. (1990). Brain magnetic resonance imaging with contrast dependent on blood oxygenation. *Proceedings of the National Academy of Sciences of the United States of America*, 87(24), 9868–9872. <https://doi.org/10.1073/pnas.87.24.9868>
- [11] Archer, J. A., Lee, A., Qiu, A., & Chen, S. H. A. (2018). Working memory, age and education: A lifespan fMRI study. *PLoS ONE*, 13(3). <https://doi.org/10.1371/journal.pone.0194878>
- [12] Liu, P., Hebrank, A. C., Rodrigue, K. M., Kennedy, K. M., Section, J., Park, D. C., & Lu, H. (2013). Age-related differences in memory-encoding fMRI responses after accounting for decline in vascular reactivity. *NeuroImage*, 78, 415–425. <https://doi.org/10.1016/j.neuroimage.2013.04.053>
- [13] Grady, C. L., McIntosh, A. R., Horwitz, B., Maisog, J. M., Ungerleider, L. G., Mentis, M. J., ... Haxby, J. V. (1995). Age-related reductions in human recognition memory due to impaired encoding. *Science*, 269(5221), 218–221. <https://doi.org/10.1126/science.7618082>
- [14] Grady, C. L., Maisog, J. M., Horwitz, B., Ungerleider, L. G., Mentis, M. J., Salerno, J. A., ... Haxby, J. V. (1994). Age-related changes in cortical blood flow activation during visual processing of faces and location. *Journal of Neuroscience*, 14(3 II), 1450–1462. <https://doi.org/10.1523/jneurosci.14-03-01450.1994>
- [15] Grady, C. L. (2008). Cognitive neuroscience of aging. *Annals of the New York Academy of Sciences*. Blackwell Publishing Inc. <https://doi.org/10.1196/annals.1440.009>
- [16] Goyal, M. S., Vlassenko, A. G., Blazey, T. M., Su, Y., Couture, L. E., Durbin, T. J., ... Raichle, M. E. (2017). Loss of Brain Aerobic Glycolysis in Normal Human Aging. *Cell Metabolism*, 26(2), 353–360.e3. <https://doi.org/10.1016/j.cmet.2017.07.010>

- [17] Al, E., Iliopoulos, F., Forschack, N., Nierhaus, T., & Grund, M. (2020). Heart – brain interactions shape somatosensory perception and evoked potentials. *ELife*, 201915629, 1–10. <https://doi.org/10.1073/pnas.1915629117>
- [18] Montoya, P., Schandry, R., & Müller, A. (1993). Heartbeat evoked potentials (HEP): topography and influence of cardiac awareness and focus of attention. *Electroencephalography and Clinical Neurophysiology/ Evoked Potentials*, 88(3), 163–172. [https://doi.org/10.1016/0168-5597\(93\)90001-6](https://doi.org/10.1016/0168-5597(93)90001-6)
- [19] Kerskens, C. M. & López Pérez, D. (2019). Cardiac-evoked long-range quantum entanglement in the conscious brain. Biorxiv. <https://doi.org/10.1101/219931>
- [20] Scholes, G. D., Fleming, G. R., Chen, L. X., Aspuru-Guzik, A., Buchleitner, A., Coker, D. F., ... Zhu, X. (2017, March 29). Using coherence to enhance function in chemical and biophysical systems. *Nature*. Nature Publishing Group. <https://doi.org/10.1038/nature21425>
- [21] Engel, G. S., Calhoun, T. R., Read, E. L., Ahn, T. K., Mančal, T., Cheng, Y. C., ... Fleming, G. R. (2007). Evidence for wavelike energy transfer through quantum coherence in photosynthetic systems. *Nature*, 446(7137), 782–786. <https://doi.org/10.1038/nature05678>
- [22] Huelga, S. F., & Plenio, M. B. (2013, July). Vibrations, quanta and biology. *Contemporary Physics*. <https://doi.org/10.1080/00405000.2013.829687>
- [23] Jedlicka, P. (2017). Revisiting the quantum brain hypothesis: Toward quantum (neuro)biology? *Frontiers in Molecular Neuroscience*, 10. <https://doi.org/10.3389/fnmol.2017.00366>
- [24] Peng, C. K., Costa, M., & Goldberger, A. L. (2009). Adaptive data analysis of complex fluctuations in physiologic time-series. *Advances in Adaptive Data Analysis*, 1(1), 61–70. <https://doi.org/10.1142/S1793536909000035>

- [25] Dos Santos, L., Barroso, J. J., De Godoy, M. F., Macau, E. E. N., & Freitas, U. S. (2014). Recurrence quantification analysis as a tool for discrimination among different dynamics classes: The heart rate variability associated to different age groups. In *Springer Proceedings in Mathematics and Statistics* (Vol. 103, pp. 125–136). Springer New York LLC. [https://doi.org/10.1007/978-3-319-09531-8\\_8](https://doi.org/10.1007/978-3-319-09531-8_8)
- [26] Zbilut, J. P., & Webber, C. L. (1992). Embeddings and delays as derived from quantification of recurrence plots. *Physics Letters A*, 171(3–4), 199–203. [https://doi.org/10.1016/0375-9601\(92\)90426-M](https://doi.org/10.1016/0375-9601(92)90426-M)
- [27] Marwan, N., & Webber, C. L. (2015). Mathematical and computational foundations of recurrence quantifications. *Understanding Complex Systems*, 3–43. <https://doi.org/10.1007/978-3-319-07155-8-1>
- [28] Wessel, N., Marwan, N., Schirdewan, A., & Kurths, J. (2003). Beat-to-beat complexity analysis before the onset of ventricular tachycardia. In *Computers in Cardiology* (Vol. 30, pp. 477–480). <https://doi.org/10.1109/cic.2003.1291196>
- [29] Censi F., Calcagnini G., Cerutti S. (2015) Dynamic Coupling Between Respiratory and Cardiovascular System. In: Webber, Jr. C., Marwan N. (eds) Recurrence Quantification Analysis. Understanding Complex Systems. Springer, Cham.
- [30] Ihlen, E. A. F. (2012). Introduction to multifractal detrended fluctuation analysis in Matlab. *Frontiers in Physiology*, 3 JUN. <https://doi.org/10.3389/fphys.2012.00141>
- [31] Lopes, R., & Betrouni, N. (2009). Fractal and multifractal analysis: A review. *Medical Image Analysis*, 13(4), 634–649. <https://doi.org/10.1016/j.media.2009.05.003>
- [32] Pereda, E., Gamundi, A., Rial, R., & González, J. (1998). Non-linear behaviour of human EEG: Fractal exponent versus correlation dimension in awake and sleep stages. *Neuroscience Letters*, 250(2), 91–94. [https://doi.org/10.1016/S0304-3940\(98\)00435-2](https://doi.org/10.1016/S0304-3940(98)00435-2)

- [33] Makowiec, D., Rynkiewicz, A., Gaaska, R., Wdowczyk-Szulc, J., & Arczyńska-Buchowiecka, M. (2011). Reading multifractal spectra: Aging by multifractal analysis of heart rate. *EPL*, 94(6). <https://doi.org/10.1209/0295-5075/94/68005>
- [34] Kehoe, E. G., Farrell, D., Metzler-Baddeley, C., Lawlor, B. A., Kenny, R. A., Lyons, D., ... Bokde, A. L. (2015). Fornix white matter is correlated with resting-state functional connectivity of the thalamus and hippocampus in healthy aging but not in mild cognitive impairment - A preliminary study. *Frontiers in Aging Neuroscience*, 7(FEB). <https://doi.org/10.3389/fnagi.2015.00010>
- [35] Alderson, T., Kehoe, E., Maguire, L., Farrell, D., Lawlor, B., Kenny, R. A., ... Coyle, D. (2017). Disrupted thalamus white matter anatomy and posterior default mode network effective connectivity in amnesic mild cognitive impairment. *Frontiers in Aging Neuroscience*, 9(NOV). <https://doi.org/10.3389/fnagi.2017.00370>
- [36] Gilligan, T. M., Sibilia, F., Farrell, D., Lyons, D., Kennelly, S. P., & Bokde, A. L. W. (2019). No relationship between fornix and cingulum degradation and within-network decreases in functional connectivity in prodromal Alzheimer's disease. *PLoS ONE*, 14(10). <https://doi.org/10.1371/journal.pone.0222977>
- [37] Robbins, T. W., James, M., Owen, A. M., Sahakian, B. J., McInnes, L., & Rabbitt, P. (1994). Cambridge neuropsychological test automated battery (CANTAB): A factor analytic study of a large sample of normal elderly volunteers. *Dementia*. <https://doi.org/10.1159/000106735>
- [38] Reitan, R. M. (1958). Validity of the Trail Making Test as an Indicator of Organic Brain Damage. *Perceptual and Motor Skills*, 8(3), 271–276. <https://doi.org/10.2466/pms.1958.8.3.271>
- [39] Arnett, J. A., & Labovitz, S. S. (1995). Effect of physical layout in performance of the Trail Making Test. *Psychological Assessment*, 7(2), 220–221. <https://doi.org/10.1037/1040-3590.7.2.220>

[40] Pignat, J. M., Koval, O., Van De Ville, D., Voloshynovskiy, S., Michel, C., & Pun, T. (2013).

The impact of denoising on independent component analysis of functional magnetic resonance imaging data. *Journal of Neuroscience Methods*, 213(1), 105–122.

<https://doi.org/10.1016/j.jneumeth.2012.10.011>

[41] Bosl, W. J., Loddenkemper, T., & Nelson, C. A. (2017). Non-linear EEG biomarker profiles for autism and absence epilepsy. *Neuropsychiatric Electrophysiology*, 3(1).

<https://doi.org/10.1186/s40810-017-0023-x>

[42] Hirata, Y., & Aihara, K. (2010). Devaney's chaos on recurrence plots. *Physical Review E - Statistical, Non-linear, and Soft Matter Physics*, 82(3).

<https://doi.org/10.1103/PhysRevE.82.036209>

[43] Marwan, N., Wessel, N., Meyerfeldt, U., Schirdewan, A., & Kurths, J. (2002). Recurrence-plot-based measures of complexity and their application to heart-rate-variability data. *Physical Review E - Statistical Physics, Plasmas, Fluids, and Related Interdisciplinary Topics*, 66(2).

<https://doi.org/10.1103/PhysRevE.66.026702>

[44] Gómez, C., & Hornero, R. (2010). Entropy and Complexity Analyses in Alzheimer's Disease: An MEG Study. *The Open Biomedical Engineering Journal*, 4(1), 223–235.

<https://doi.org/10.2174/1874120701004010223>

[45] Kennel, M. B., Brown, R., & Abarbanel, H. D. I. (1992). Determining embedding dimension for phase-space reconstruction using a geometrical construction. *Physical Review A*, 45(6), 3403–3411. <https://doi.org/10.1103/PhysRevA.45.3403>

[46] Marwan, N., Carmen Romano, M., Thiel, M., & Kurths, J. (2007, January). Recurrence plots for the analysis of complex systems. *Physics Reports*.

<https://doi.org/10.1016/j.physrep.2006.11.001>

- [47] Roulston, M. S. (1999). Estimating the errors on measured entropy and mutual information. *Physica D: Non-linear Phenomena*, 125(3–4), 285–294.  
[https://doi.org/10.1016/S0167-2789\(98\)00269-3](https://doi.org/10.1016/S0167-2789(98)00269-3)
- [48] Thiel, M., Romano, M. C., Kurths, J., Meucci, R., Allaria, E., & Arecchi, F. T. (2002). Influence of observational noise on the recurrence quantification analysis. *Physica D: Non-linear Phenomena*, 171(3), 138–152. [https://doi.org/10.1016/S0167-2789\(02\)00586-9](https://doi.org/10.1016/S0167-2789(02)00586-9)
- [49] Ma, Q., Ning, X., Wang, J., & Bian, C. (2006). A new measure to characterize multifractality of sleep electroencephalogram. *Chinese Science Bulletin*, 51(24), 3059–3064.  
<https://doi.org/10.1007/s11434-006-2213-y>
- [50] Dick, O. E., & Svyatogor, I. A. (2012). Potentialities of the wavelet and multifractal techniques to evaluate changes in the functional state of the human brain. *Neurocomputing*, 82, 207–215. <https://doi.org/10.1016/j.neucom.2011.11.013>
- [51] Ho, P.S, Lin, C., Chen, G. Y., Liu, H. L., Huang, C.M., Lee, T.M., Lee, S.H., & Wu, S.C. (2017). Complexity analysis of resting state fMRI signals in depressive patients. *Conference proceedings : ... Annual International Conference of the IEEE Engineering in Medicine and Biology Society. IEEE Engineering in Medicine and Biology Society. Annual Conference, 2017*, 3190–3193. <https://doi.org/10.1109/EMBC.2017.8037535>
- [52] Manor, B., & Lipsitz, L. A. (2013). Physiologic complexity and aging: Implications for physical function and rehabilitation. *Progress in Neuro-Psychopharmacology and Biological Psychiatry*, 45, 287–293. <https://doi.org/10.1016/j.pnpbp.2012.08.020>
- [53] Guttmann, C. R., Jolesz, F. A., Kikinis, R., Killiany, R. J., Moss, M. B., Sandor, T., & Albert, M. S. (1998). White matter changes with normal aging. *Neurology*, 50(4), 972-978.

- [54] Gunning-Dixon, F. M., & Raz, N. (2003). Neuroanatomical correlates of selected executive functions in middle-aged and older adults: a prospective MRI study. *Neuropsychologia*, 41(14), 1929-1941.
  
- [55] Provyn, J. P., Sliwinski, M. J., & Howard, M. W. (2007). Effects of Age on Contextually Mediated Associations in Paired Associate Learning. *Psychology and Aging*, 22(4), 846–857. <https://doi.org/10.1037/0882-7974.22.4.846>
  
- [56] Sala-Llloch, R., Bartrés-Faz, D., & Junqué, C. (2015). Reorganization of brain networks in aging: a review of functional connectivity studies. *Frontiers in Psychology*, 6. <https://doi.org/10.3389/fpsyg.2015.00663>
  
- [57] Feinberg, D. A., Moeller, S., Smith, S. M., Auerbach, E., Ramanna, S., Glasser, M. F., ... Yacoub, E. (2010). Multiplexed echo planar imaging for sub-second whole brain fmri and fast diffusion imaging. *PLoS ONE*, 5(12). <https://doi.org/10.1371/journal.pone.0015710>



# Tables

<i>Parameter</i>	<i>Young</i>	<i>Old</i>
<b><i>Det</i></b>	32.16 ± 10.12	35.72 ± 11.99
<b><i>MeanLine*</i></b>	2.81 ± .34	3.07 ± .51
<b><i>MaxLine**</i></b>	99.10 ± 38.35	135.53 ± 58.63
<b><i>Ent*</i></b>	.77 ± .19	.92 ± .24
<b><i>Lam**</i></b>	35.42 ± 8.24	46.50 ± 14.00
<b><i>TT***</i></b>	2.24 ± .11	2.48 ± .26
<b><i>W***</i></b>	.15 ± .08	.27 ± .07
<b><i>H***</i></b>	.02 ± .01	.03 ± .01

**Table 1.** Group mean averages of the RQA and MFDFA parameters extracted from the ZQC weighted time-series for the young and old groups ( $p < .05(*)$ ,  $p < .01(**)$ ,  $p < .001(***)$ ).

<i>Parameter</i>	<i>QC max movement</i>	<i>QC mean movement</i>
<b><i>Det</i></b>	-.36 (.07)	.13 (.50)
<b><i>MeanLine</i></b>	-.10 (.60)	.00 (.97)
<b><i>MaxLine</i></b>	-.30 (.13)	-.01 (.95)
<b><i>Ent</i></b>	-.26 (.19)	.08 (.69)
<b><i>Lam</i></b>	-.27 (.17)	.17 (.38)
<b><i>TT</i></b>	-.13 (.52)	.22 (.27)
<b><i>W</i></b>	.06 (.77)	.02 (.92)
<b><i>H</i></b>	-.14 (.47)	-.06 (.77)

**Table 2.** Spearman correlations between quality control movement measures from the rs-fMRI session and the non-linear parameters of the ZQC signals. In these correlations,  $n$  was equal to 27 since movement information was not available for one participant and another did not pass quality control (see section 2.5).

<i>Parameter</i>	<i>Pat. Recognition Mem. (immediate recall)</i>	<i>Paired Associates Learning</i>	<i>Spat. working Mem. (strategy)</i>	<i>Pat. Recognition Mem. (delayed recall)</i>	<i>Trial A</i>	<i>Trial B</i>
<b><i>Det</i></b>	<b>-0.31 (.01)*</b>	.06 (.62)	-.19 (.13)	-.02 (.87)	.05 (.69)	-.02 (.87)
<b><i>MeanLine</i></b>	<b>-0.33 (.009)**</b>	-.04 (.71)	-.17 (.17)	-.13 (.31)	.00 (.98)	-.04 (.74)
<b><i>MaxLine</i></b>	<b>-0.34 (.008)**</b>	-.18 (.16)	<b>-0.26 (.04)*</b>	-.19 (.12)	-.00 (.96)	-.02 (.86)
<b><i>Ent</i></b>	<b>-0.33 (.009)**</b>	.06 (.65)	-.21 (.10)	-.12 (.33)	.09 (.49)	-.04 (.76)
<b><i>Lam</i></b>	<b>-0.29 (.02)*</b>	.03 (.78)	<b>-0.34 (.008)**</b>	-.09 (.48)	-.04 (.72)	-.05 (.68)
<b><i>TT</i></b>	-.25 (.05)+	-.08 (.51)	<b>-0.29 (.02)*</b>	-.18 (.15)	.01 (.90)	-.07 (.57)
<b><i>W</i></b>	-.18 (.14)	-.04 (.71)	-.13 (.29)	-.17 (.17)	.25 (.06)+	.13 (.31)
<b><i>H</i></b>	-.24 (.06)+	.04 (.75)	-.22 (.10)	-.09 (.48)	.00 (.95)	.07 (.60)

*Table 3. Spearman correlations between the non-linear parameters of the ZQC signals and the CANTAB and TNT scores. In these correlations, n varies between 59 (CANTAB scores) and 55 (TNT scores) since one participant did not pass quality control (see section 2.5) and the measures were not available to all of them. p-values are in parenthesis (trend (+)  $p < .05$ (\*) and  $p < .01$ (\*\*)).*

## Figures



**Figure 1.** Acquisition model which includes the image slice (central red line) and the REST slabs above and below the imaging slice both 5 mm thick and separated 15 mm and 20 mm

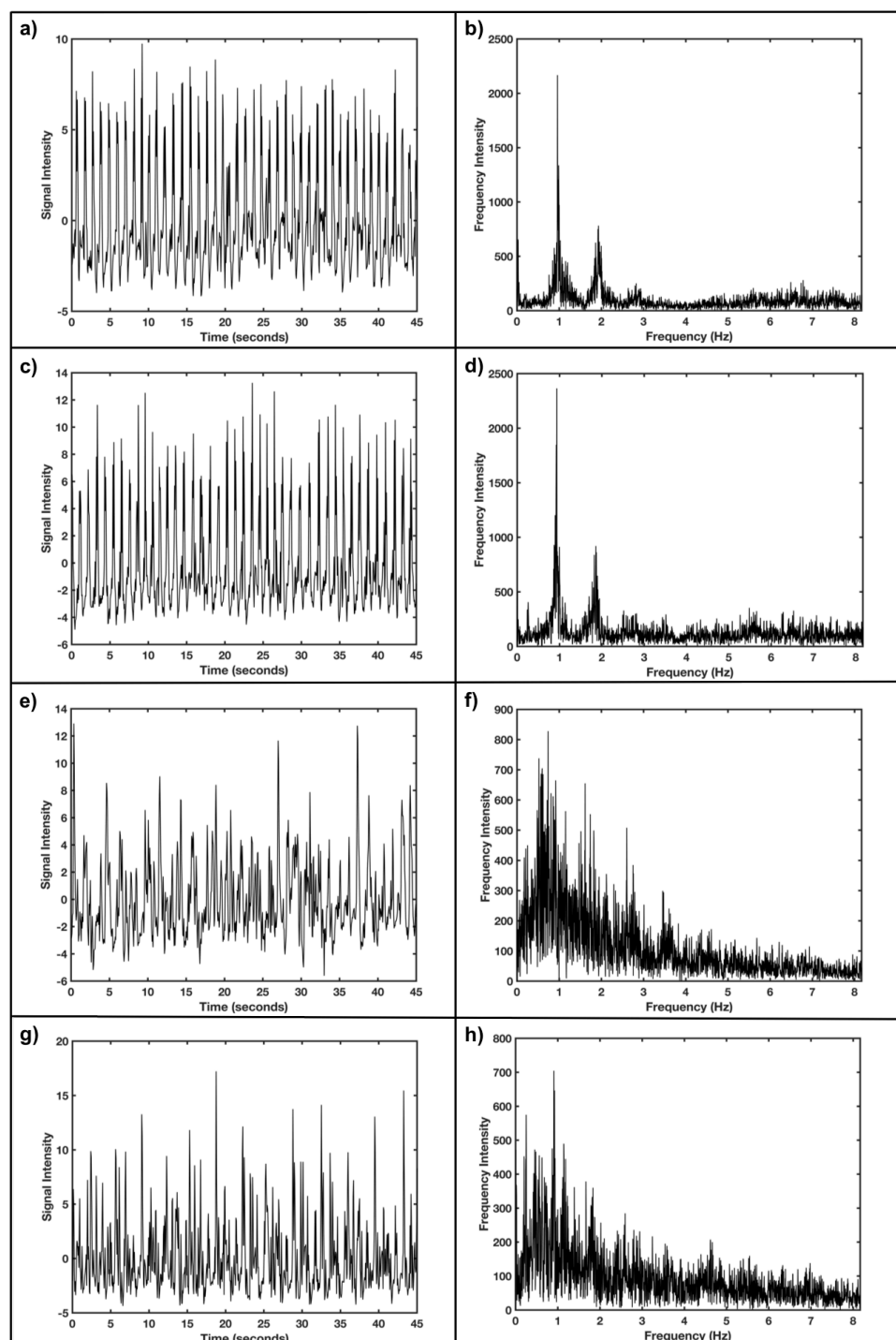


**Figure 2.** Example of the time-series as well as its frequency spectra for two young (a-c and b-d) and two healthy old adults (e-g and f-h). These examples are representing the typical results

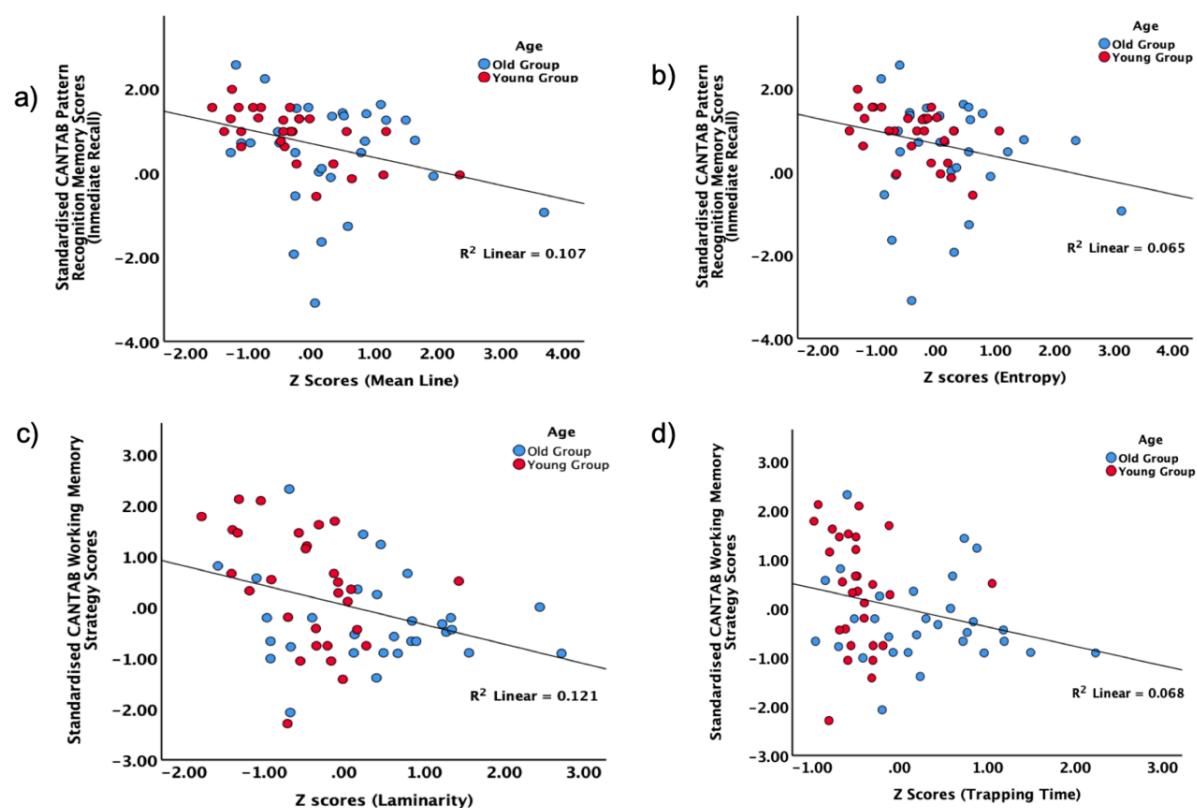


**Figure 3.** Examples of linear regressions between mean line (a) and entropy(b), and Standardised CANTAB Pattern Recognition Memory Scores (Immediate Recall), and between Laminarity (c) and Trapping Time (d), and standardised CANTAB working memory strategy scores.